Dalton Transactions

Cite this: *Dalton Trans.*, 2012, **41**, 3154

www.rsc.org/dalton

PAPER

Exploring hypervalency and three-centre, four-electron bonding interactions: Reactions of acenaphthene chalcogen donors and dihalogen acceptors†

Fergus R. Knight, Kasun S. Athukorala Arachchige, Rebecca A. M. Randall, Michael Bühl, Alexandra M. Z. Slawin and J. Derek Woollins*

Received 25th October 2011, Accepted 15th December 2011
DOI: 10.1039/c2dt12031c

Sterically crowded *peri*-substituted selenium and tellurium acenaphthene donors **D1–D7** [Acenap(EPh)(Br) E = Se, Te; Acenap(SePh)(EPh) E = Se, S; Acenap(TePh)(EPh) E = S, Se, Te] react with dibromine and diiodine acceptors to afford a group of structurally diverse addition products **1–12**, comparable in some cases to previously reported naphthalene analogues. Tellurium donors **D4–D6** react conventionally with the dihalogens to afford insertion adducts **6–11** (X-R_2Te-X) exhibiting molecular see-saw geometries, characterised by *hypervalent* X-Te-X *quasi*-linear fragments. The reactions of selenium donors **D1–D3** with diiodine afford expected neutral charge-transfer (CT) spoke adducts **1**, **4** and **5** (R_2Se-I-I) containing *quasi*-linear Se-I-I alignments. Conversely, treatment of **D2** and **D3** with dibromine results in the formation of two tribromide salts **2** and **3** containing bromoselanyl cations $[R_2Se–Br]^+\cdots[Br–Br_2]^-$, each exhibiting a *quasi*-linear three-body Br–Se···E (E = Se, S) fragment. The *peri*-bonding in these species can be thought of as a weak *hypervalent* G···Se-X three-centre, four-electron (3c-4e) type interaction, closely related to the T-shaped 3c-4e interaction. Density-functional calculations performed on **2** and **3** and their bare cations (**2a** and **3a**) reveal Wiberg bond indices of 0.25–0.37, suggesting substantial 3c-4e character in these systems. The presence of such an interaction operating in **2** and **3** alleviates steric strain within the *peri*-region and minimises the degree of molecular distortion required to achieve a relaxed geometry. Ditellurium donor **D7** reacts with dibromine to afford an unorthodox insertion adduct **12** containing a Te–O–Te bridge and two *quasi*-linear Br–Te–O fragments, with the central tellurium atoms assuming a molecular see-saw geometry. Whilst DFT calculations indicate **12** is thermodynamically unfavourable, its formation is viable under experimental conditions.

Introduction

The interaction of atoms is an integral aspect of chemistry, biology and materials science. The pioneering work on the electronic theory of the covalent bond by Lewis and Langmuir in the early 1900s,[1] led to great advances in the area of strong bonding (covalent/ionic), but the ambiguity over "*hypervalent*" species[1–4] and the nature of weak, non-covalent interactions,[5,6] continues to intrigue chemists. The search for structures which invoke new and unusual types of interactions is therefore indispensible for developing our understanding of non-bonded forces and the theory of bonding.

Organo-Group 16 donor compounds react with dihalogen (I_2, Br_2) and interhalogen (IBr, ICl) acceptors to afford addition complexes containing unconventional bonding situations.[7–9] A wide variety of structural archetypes are known, of which the neutral charge-transfer (CT) spoke adduct (R_2E-X-Y, 10-X-2) and the see-saw insertion adduct (X-ER_2-Y, 10-E-4) are the most common.[7–10] Experimental factors such as the type of chalcogen donor atom, the form of the dihalogen or inter-halogen, the stoichiometry of the reactants and the nature of the donor atoms' R group(s) all play a significant role and control the reaction pathway.[7–10]

Spoke and see-saw conformations of RR′E·X_2 type adducts are predicted to be in equilibrium in solution, with reactions between chalcogen donors [R_2E] and di- and interhalogens progressing *via* nucleophilic attack at either the halogen or chalcogen site of a common $[R_2E\text{-}X]^+$ cation intermediate.[7–9,11–14] The conformation of the final structure is thus dictated by the degree of charge-transfer from non-bonding chalcogen donor orbitals *n*(E) to the LUMO of the di- or inter-halogen acceptor σ^*(X-X′). Typically, see-saw adducts are formed when halide X is more electronegative than chalcogen E $[R_2E^{\delta+}\text{-}X^{\delta-}]$, with nucleophilic halide attack occurring at the chalcogen atom.[7–10,12,15]

The defining *quasi*-linear E-X-Y and X-E-Y fragments of spoke and see-saw adducts, appear to violate the octet rule and

EaSTCHEM School of Chemistry, University of St Andrews, St Andrews, Fife, U.K.. E-mail: jdw3@st-andrews.ac.uk; Fax: (+44) 1334 463384; Tel: (+44)1334 463861

† Electronic supplementary information (ESI) available: Full experimental details, computaional methods and tables, X-ray crystal structure data. CCDC reference numbers 850816–850827. For ESI and crystallographic data in CIF or other electronic format see DOI: 10.1039/c2dt12031c

are thus classified as *hypervalent*.[1] *Hypervalency* of the heavier main group elements has been debated upon since the innovative work by Langmuir and Lewis[1] and remains an area of contention to chemists. The advancement of molecular orbital theory, led Rundle and Pimentel to develop the work by Sugden[2] and introduce the notion of a three centre four-electron bond (3c-4e).[2] This concept has evolved to include related four- and five-centre, six electron bonds (4c, 6e; 5c, 6e)[9] and continues to be a favoured method for explaining *hypervalency* without violating the octet rule or invoking ionic bonding.[4] Numerous compounds containing linear fragments have been well documented[7–9,16] with the nature of the bonding described by the Rundle–Pimentel 3c-4e model and a charge-transfer model.[2,17]

We have previously utilised the rigidity of polycyclic aromatic hydrocarbons, naphthalene[18] and related 1,2-dihydroacenaphthylene (acenaphthene),[19] to constrain bulky heteroatoms in unavoidably congested environments, at distances within the sum of the van der Waals radii. The geometric constraints unique to these frameworks, imposed by a double substitution of atoms or groups at the *peri*-positions, offer good scaffolds with which to study non-bonded intramolecular interactions.[5,6,18–22]

Initially we focused on naphthalene, investigating dichalcogenide[23] ligands and unusual phosphorus compounds[24] before expanding our research to mixed phosphorus-chalcogen,[25] chalcogen-chalcogen[26–28] and halogen-chalcogen[29] systems. More recently we have exploited the acenaphthene backbone to prepare corresponding halogen-chalcogen and chalcogen-chalcogen derivatives.[30]

During our investigations of *peri*-substituted naphthalenes we prepared a number of chalcogen-donors[26,29] and reported their reactions with dibromine and diiodine.[27] The structurally diverse array of addition adducts exhibited a number of linear fragments which were classified as hypervalent and represented by the Rundle–Pimentel 3c-4e model.[2,17,27] *Hypervalency* is a topic of continued interest, with the quest for linear arrangements a common priority for tracing hypercoordinate interactions. The work presented here complements our previous study, reporting an investigation of related acenaphthene chalcogen donor compounds **D1–D7** and their reactions with dibromine and diiodine.

Results and discussion

Compounds **1–12** were synthesised and characterised by multinuclear NMR and IR spectroscopy and mass spectrometry. The homogeneity of the new compounds was, where possible, confirmed by microanalysis. ^{77}Se and ^{125}Te NMR spectroscopy data is displayed in Table 1. Suitable single crystals were obtained for **1–12** by diffusion of hexane into saturated solutions of the individual compound in dichloromethane. The molecular structures of **1–12** are analysed together here and compared with the structures of acenaphthene donors **D1–D7**[30] and previously reported analogous naphthalene addition adducts.[27] Compounds **1–10** crystallise with one molecule in the asymmetric unit, compounds **11** and **12** contain two nearly identical molecules in the asymmetric unit. Selected interatomic distances, angles and torsion angles are listed in Tables 2 and 3. Further crystallographic information can be found in Tables 4–6 and in the Electronic Supporting Information (ESI)†.

Neutral charge-transfer (CT) spoke adducts (R_2E-X-X) are formed whenever there is a weak coordination involving a transfer of electron density from non-bonding chalcogen orbitals into the LUMO of the halogen acceptor molecule.[7–9,12,15] The degree of charge transfer can be predicted from electronegativity (χ) values, with CT adducts generally formed when χ(X) is less than χ(E).[7–9,12,15] Upon CT formation there is a natural lowering of the dihalogen bond order and a lengthening of the X-X bond.[7,8] Strong adducts are characterised by X···X bond orders in the range 0.4–0.6 and contain E-X-X three body fragments.[7] Even stronger interactions between the chalcogen donor and the dihalogen acceptor, results in the cleavage of the X-X bond and leads to the formation of an $[R_2E\text{-}X]^+$ cation which interacts with a X^- anion.[7] In this instance, the X-X CT bond is considered an $X^+\cdots X^-$ ionic interaction, with bond orders less than 0.4 and X···X separations larger than the sum of van der Waals radii.[7]

Whilst the majority of CT adducts structurally characterised in the literature are prepared from organosulfur donors[7,8,10,31] [χ(S) 2.58][32] and diiodine [χ(I) 2.36],[32] the "softer" character of organoselenides [χ(Se) 2.35],[32] which implies greater donor properties compared with sulfur, results in significantly stronger adducts exhibiting elongated iodine–iodine bond lengths.[7,8,33]

Selenium donor compounds **D1**, **D2** and **D3** react conventionally[7,8,27,30] with a single equivalent of diiodine to afford similar CT spoke adducts (**1**, **4** and **5** respectively; Scheme 1, Fig. 1), exhibiting *quasi*-linear Se-I-I fragments [Se-I-I angles 171–173°; Table 3]. The ^{77}Se NMR spectra for **1** [δ = 437.6 ppm], **4** [δ = 421.0 ppm] and **5** [δ = 460.4 ppm] display the expected downfield shifts, compared with donor compounds **D1** [δ = 423.7 ppm], **D2** [δ = 408.3 ppm] and **D3** [δ = 433.7 ppm],

Table 1 ^{77}Se and ^{125}Te NMR spectroscopic data[a]

	1	**2**	**3**	**4**	**5**		
Peri-atoms	Se, Br	Se, Se	Se, S	Se, Se	Se, S		
Linear arrangement	Se–I–I	Br–Se–Se	Br–Se–S	Se–I–I	Se–I–I		
^{77}Se NMR	437.6	405.2	431.2	421	460.4		
	6	**7**	**8**	**9**	**10**	**11**	**12**
Peri-atoms	Te, Br	Te, Br	Te, S	Te, Se	Te, S	Te, Se	Te, Te
Linear arrangement	Br–Te–Br	I–Te–I	Br–Te–Br	Br–Te–Br	I–Te–I	I–Te–I	Br–Te–O
^{77}Se NMR	—	—	—	332.9	—	343.2	—
^{125}Te NMR	918.8	860.6	930.6	921.9	878.9	871	961.3

[a] Spectrum of **1** run in CD_3CN, spectra of **2** and **3** run in $(CD_3)_2CO$, spectra of **4–11** run in $CDCl_3$, spectrum of **12** run in $(CD_3)_2NCOD$; δ (ppm).

Table 2 Selected interatomic distances [Å] and angles [°] for compounds **1–12**

Compound	**1**	**2**	**3**	**4**	**5**	**6**
Peri-moieties	Br SePhI$_2$	BrSePh SePh	BrSePh SPh	I$_2$SePh SePh	I$_2$SePh SPh	Br TePhBr$_2$
Peri-region distances and sub-van der Waals contacts						
E(1)···X/E	3.1753(19)	2.801(3)	2.740(3)	3.326(3)	3.252(2)	3.2581(19)
% Σr_{vdW}[a]	85	74	74	88	88	83
Peri-region bond angles						
E(1)–C(1)–C(10)	122.3(9)	117.2(14)	118.0(6)	122.6(11)	123.4(5)	122.8(10)
C(1)–C(10)–C(9)	133.6(11)	132(2)	129.5(8)	132.6(13)	132.5(6)	132.0(12)
X/E–C(9)–C(10)	120.8(9)	118.1(15)	117.9(6)	125.3(11)	123.1(6)	120.0(9)
Σ of bay angles	376.7(24)	367.3(39)	365.4(16)	380.5(29)	379.0(14)	374.8(25)
Splay angle[b]	16.7	7.3	5.4	20.5	19	14.8
Out-of-plane displacement						
E(1)	0.125(1)	−0.073(1)	0.069(1)	−0.091(1)	0.130(1)	0.531(1)
X/E(1)	−0.101(1)	0.121(1)	−0.163(1)	0.179(1)	−0.133(1)	−0.205(1)
Central acenaphthene ring torsion angles						
C:(6)–(5)–(10)–(1)	178.85(1)	179.29(1)	−178.60(1)	−179.55(1)	178.01(1)	174.62(1)
C:(4)–(5)–(10)–(9)	179.14(1)	−176.49(1)	177.79(1)	−178.75(1)	178.30(1)	−179.67(1)
Compound	**7**	**8**	**9**	**10**	**11**	**12**
Peri-moieties	Br TePhI$_2$	Br$_2$TePh SPh	Br$_2$TePh SePh	I$_2$TePh SPh	I$_2$TePh SePh	(BrTePh)$_2$O
Peri-region distances and sub-van der Waals contacts						
E(1)···X/E	3.2050(11)	3.218(3)	3.2729(8)	3.141(4)	3.2677(18) [3.2862(18)]	3.335(1) [3.385(1)]
% Σr_{vdW}[a]	82	83	83	81	83 [83]	81 [82]
Peri-region bond angles						
E(1)–C(1)–C(10)	123.2(4)	121.8(10)	123.6(5)	122.8(8)	124.4(8) [122.3(8)]	124.0(3) [123.2(4)]
C(1)–C(10)–C(9)	131.8(5)	132.2(14)	131.1(7)	129.0(11)	128.7(9) [131.7(10)]	132.1(4) [132.3(4)]
X/E–C(9)–C(10)	121.8(4)	121.7(10)	122.6(5)	122.7(10)	122.2(7) [121.6(9)]	122.9(3) [124.6(3)]
Σ of bay angles	376.8(11)	375.7(27)	377.3(14)	374.5(23)	375.3(19) [375.6(22)]	379.0(8) [380.1(9)]
Splay angle[b]	16.8	15.7	17.3	14.5	15.3 [15.6]	19.0 [20.1]
Out-of-plane displacement						
E(1)	−0.055(1)	0.493(1)	−0.447(1)	0.122(1)	−0.463(1) [−0.582(1)]	0.045(1) [0.099(1)]
X/E(1)	0.154(1)	−0.257(1)	0.217(1)	0.162(1)	0.487(1) [0.402(1)]	−0.139(1) [0.115(1)]
Central acenaphthene ring torsion angles						
C:(6)–(5)–(10)–(1)	179.52(1)	176.92(1)	−175.53(1)	−179.00(1)	−175.72(1) [−176.60(1)]	179.78(1) [179.01(1)]
C:(4)–(5)–(10)–(9)	−177.77(1)	175.99(1)	−177.49(1)	178.10(1)	175.82(1) [−172.96(1)]	176.60(1) [178.03(1)]

[a] van der Waals radii used for calculations: r_{vdW}(S) 1.80 Å, r_{vdW}(Se) 1.90 Å, r_{vdW}(Te) 2.06 Å, r_{vdW}(Br) 1.85 Å;[34] [b] Splay angle: Σ of the three bay region angles −360.

Table 3 Selected interatomic Se–I–I, Br–Se–E′, Br–Br–Br, X–Te–X and Br–Te–O distances [Å] and angles [°] for **1–12**

Compound	**1**	**4**	**5**		**2**	**3**
Se(1)–I(1)	2.9565(17)	2.901(2)	2.9102(12)	Se(1)–Br(1)	2.458(3)	2.4409(17)
I(1)–I(2)	2.8161(14)	2.8267(19)	2.8168(10)	Se(1)—E(2)	2.801(3)	2.740(3)
				Br(2)–Br(3)	2.518(4)	2.614(2)
				Br(3)–Br(4)	2.582(4)	2.502(2)
Se(1)–I(1)–I(2)	171.32(4)	173.22(6)	173.16(3)	Br(1)–Se(1)–E(2)	171.42(11)	174.95(1)
				Br(2)–Br(3)–Br(4)	178.19(9)	179.24(5)
Compound	**6**	**7**	**8**	**9**	**10**	**11**
Te(1)–X(1)	2.7025(17)	2.9613(8)	2.6766(17)	2.6808(9)	2.8860(19)	2.9630(14) [2.9327(13)]
Te(1)–X(2)	2.6583(19)	2.9199(8)	2.6850(17)	2.6859(9)	2.9648(19)	2.8976(14) [2.9173(14)]
X(1)–Te(1)–X(2)	174.23(6)	173.04(2)	175.49(5)	175.54(3)	177.73(4)	177.18(4) [177.67(4)]
Compound	**12**					
Br(1)–Te(1)	2.8261(7) [3.024(3)]		Te(2)–O(1)	1.992(3) [2.045(3)]		
Te(1)–O(1)	2.005(3) [1.942(3)]		Te(2)–Br(2)	2.8862(7) [2.7654(7)]		
Br(1)–Te(1)–O(1)	176.46(8) [174.73(8)]		Br(2)–Te(2)–O(1)	172.52(9) [175.41(9)]		

respectively (Table 1).[30] In all three derivatives, coordination of selenium to the diiodine molecule results in a reduction of bond order, of the I–I bond, which extends from 2.66 Å (free iodine)[35] to an average 2.82 Å (Table 3). CT spoke adducts are classified by the directional parameter θ, which calculates the position of the E-X vector, with respect to the plane containing the chalcogen two electron-pairs in a tetrahedral sp^3 geometry (Fig. 2).[7] In **1**, **4** and **5**, the diiodine molecule lies *quasi*-perpendicular to the R$_2$Se plane, with dihedral angles 69–79°, indicative of donor molecules having sterically crowded chalcogen lone-pairs.[7]

Upon the formation of CT spoke **1**, there is no significant alteration in the acenaphthene geometry compared with the structure of donor **D1**.[30] The phenyl ring orientates with a similar equatorial conformation, aligning the Se–C$_{Ph}$ bond along the mean plane, corresponding to a type B configuration (Fig. 3).[36] Molecular distortion and by inference the *peri*-distance, is comparable in both donor and adduct, with non-bonded

Table 4 Crystallographic data for compounds **1–4**

	1	**2**	**3**	**4**
Empirical formula	$C_{18}H_{13}BrI_2Se$	$C_{24}H_{18}Br_6Se_2$	$C_{24.25}H_{18.5}Br_4Cl_{0.5}SSe$	$C_{24}H_{18}Se_2I_2$
Formula weight	641.97	943.75	758.28	718.14
T/°C	−148(1)	−148(1)	−148(1)	−148(1)
Crystal colour, habit	red, platelet	orange, chip	red, platelet	colourless, prism
Crystal dimensions (mm^3)	0.210 × 0.090 × 0.020	0.150 × 0.060 × 0.030	0.240 × 0.170 × 0.030	0.20 × 0.20 × 0.20
Crystal system	Monoclinic	Triclinic	Triclinic	Monoclinic
Lattice parameters	a = 14.174(7) Å	a = 10.870(5) Å	a = 10.822(8) Å	a = 9.555(5) Å
	b = 14.165(7) Å	b = 11.404(6) Å	b = 11.568(8) Å	b = 8.242(4) Å
	c = 9.265(5) Å	c = 11.938(6) Å	c = 11.940(10) Å	c = 28.147(14) Å
	—	α = 106.223(7)°	α = 81.42(3)°	—
	β = 106.194(10)°	β = 91.894(8)°	β = 73.07(3)°	β = 97.390(13)°
	—	γ = 108.294(9)°	γ = 71.07(3)°	—
Volume/Å^3	V = 1787(2)	V = 1337.3(11)	V = 1350.2(17)	V = 2198.4(20)
Space group	P21/c	$P\bar{1}$	$P\bar{1}$	P21/n
Z value	4	2	2	4
D_{calc} (g cm^{-3})	2.387	2.344	1.865	2.17
F_{000}	1184	880	725	1344
μ(Mo-Kα)/cm^{-1}	77.97	117.691	74.64	1.822
No. of reflections measured	13238	11213	11677	18239
R_{int}	0.0869	0.0849	0.0707	0.1087
Min. and max. transmissions	0.341–0.856	0.348–0.703	0.528–0.799	0.152–0.290
Observed reflection (no. variables)	3140(199)	5355(289)	4740(293)	5113(253)
Reflection/parameter ratio	15.78	18.53	16.18	20.21
Residuals: R_1 ($I > 2.00\sigma(I)$)	0.0493	0.1066	0.0866	0.0952
Residuals: R (all reflections)	0.0605	0.147	0.1292	0.1343
Residuals: wR_2 (all reflections)	0.1936	0.3337	0.2791	0.3043
Goodness of fit indicator	1.022	1.203	1.059	1.274
Maximum peak in final diff. map	1.81 e$^-$/Å^3	2.46 e$^-$/Å^3	1.64 e$^-$/Å^3	2.29 e$^-$/Å^3
Minimum peak in final diff. map	−2.05 e$^-$/Å^3	−2.40 e$^-$/Å^3	−1.27 e$^-$/Å^3	−2.48 e$^-$/Å^3

Table 5 Crystallographic data for compounds **5–8**

	5	**6**	**7**	**8**
Empirical formula	$C_{24}H_{18}I_2SSe$	$C_{18}H_{13}Br_3Te$	$C_{18}H_{13}BrI_2Te$	$C_{24}H_{18}Br_2STe$
Formula weight	671.24	596.61	690.61	625.87
T/°C	−148(1)	−148(1)	−148(1)	−148(1)
Crystal colour, habit	red, platelet	yellow, chip	orange/red, platelet	yellow, chunk
Crystal dimensions (mm^3)	0.240 × 0.040 × 0.020	0.24 × 0.15 × 0.06	0.24 × 0.06 × 0.03	0.150 × 0.120 × 0.030
Crystal system	Monoclinic	Orthorhombic	Monoclinic	Monoclinic
Lattice parameters	a = 9.578(4) Å	a = 15.745(7) Å	a = 26.071(7) Å	a = 12.516(5) Å
	b = 8.184(3) Å	b = 10.066(4) Å	b = 9.378(2) Å	b = 12.616(5) Å
	c = 28.084(10) Å	c = 22.162(9) Å	c = 15.682(4) Å	c = 14.436(6) Å
	—	—	—	—
	β = 96.485(9)°	—	β = 105.281(5)°	β = 112.682(8)°
	—	—	—	—
Volume/Å^3	V = 2187.4(13)	V = 3512(3)	V = 3698.4(16)	V = 2103(2)
Space group	P21/n	Pbcn	$C2/c$	P21/n
Z value	4	8	8	4
D_{calc} (g cm^{-3})	2.038	2.256	2.48	1.977
F_{000}	1272	2224	2512	1200
μ(Mo-Kα)/cm^{-1}	46.443	85.335	71.107	53.334
No. of reflections measured	15951	26513	14642	15436
R_{int}	0.0473	0.1228	0.0415	0.1181
Min. and max. transmissions	0.448–0.911	0.308–0.599	0.418–0.808	0.425–0.852
Observed reflection (no. variables)	3848(253)	3563(199)	3729(199)	3692(253)
Reflection/parameter ratio	15.21	17.9	18.74	14.59
Residuals: R_1 ($I > 2.00\sigma(I)$)	0.0411	0.0801	0.0379	0.0956
Residuals: R (all reflections)	0.0529	0.0988	0.0468	0.1257
Residuals: wR_2 (all reflections)	0.1625	0.2488	0.149	0.2865
Goodness of fit indicator	1.215	1.405	1.267	1.347
Maximum peak in final diff. map	1.66 e$^-$/Å^3	1.39 e$^-$/Å^3	2.67 e$^-$/Å^3	1.99 e$^-$/Å^3
Minimum peak in final diff. map	−1.76 e$^-$/Å^3	−1.62 e$^-$/Å^3	−2.88 e$^-$/Å^3	−2.23 e$^-$/Å^3

Se···Br separations for **1** [3.1753(19) Å] and **D1** [3.1588(16) Å][30] ∼15% shorter than the sum of van der Waals radii. Maximum C–C–C–C central acenaphthene ring torsion angles indicate greater planarity in the organic backbone upon diiodine coordination, with deviation by ∼1° compared with 3–5° in **D1**.[30]

Table 6 Crystallographic data for compounds **9–12**

	9	**10**	**11**	**12**
Empirical formula	$C_{24}H_{18}SeTeBr_2$	$C_{24}H_{18}I_2STe$	$C_{24.05}H_{18.10}Cl_{0.1}I_2SeTe$	$C_{25.5}H_{21.5}Br_2N_{0.5}O_{1.5}Te_2$
Formula weight	672.77	719.88	770.99	773.96
T/°C	−148(1)	−148(1)	−148(1)	−148(1)
Crystal colour, habit	yellow, prism	brown, chunk	orange, platelet	colourless, prism
Crystal dimensions (mm^3)	0.15 × 0.15 × 0.06	0.150 × 0.150 × 0.020	0.09 × 0.03 × 0.03	0.150 × 0.150 × 0.150 mm
Crystal system	Monoclinic	Monoclinic	Triclinic	Monoclinic
Lattice parameters	a = 12.680(4) Å	a = 11.129(6) Å	a = 11.079(3) Å	a = 11.599(3) Å
	b = 12.776(3) Å	b = 16.603(9) Å	b = 14.105(4) Å	b = 23.952(6) Å
	c = 14.386(4) Å	c = 12.582(7) Å	c = 16.134(5) Å	c = 17.983(4) Å
	—	—	α = 82.21(2)°	—
	β = 113.068(6)°	β = 102.416(10)°	β = 78.41(2)°	β = 95.095(7)°
	—	—	γ = 77.42(2)°	—
Volume/Å^3	V = 2144.2(10)	V = 2270(2)	V = 2399.4(12)	V = 4976(2)
Space group	$P2_1/n$	P21/n	$P\bar{1}$	P21/n
Z value	4	4	4	8
D_{calc} (g cm^{-3})	2.084	2.106	2.134	2.066
F_{000}	1272	1344	1424	2912
μ(Mo-Kα)/cm^{-1}	68.314	41.306	53.49	55.861
No. of reflections measured	16726	18531	19966	31149
R_{int}	0.0473	0.102	0.0619	0.0472
Min and max transmissions	0.419–0.664	0.208–0.921	0.310–0.852	0.347–0.433
Observed reflection (no. variables)	4324(253)	4609(253)	9555(516)	9013(568)
Reflection/parameter ratio	17.09	18.22	17.96	15.87
Residuals: R_1 ($I > 2.00\sigma(I)$)	0.0453	0.0758	0.0664	0.0329
Residuals: R (all reflections)	0.0535	0.1013	0.0941	0.0403
Residuals: wR_2 (all reflections)	0.1624	0.2485	0.2394	0.0692
Goodness of fit indicator	1.129	1.287	1.205	1.081
Maximum peak in final diff. map	1.58 e$^-$/Å^3	1.94 e$^-$/Å^3	2.60 e$^-$/Å^3	0.95 e$^-$/Å^3
Minimum peak in final diff. map	−1.79 e$^-$/Å^3	−2.58 e$^-$/Å^3	−3.21 e$^-$/Å^3	−0.76 e$^-$/Å^3

The *quasi*-linear Se-I-I fragment resides above the *peri*-gap at 92.24(1)° to the Se(1)–C(13) bond and 69.23(1)° to the C(13)–Se(1)–C(1) plane (Fig. 2). The equatorial configuration of the type B structure reduces the interaction between repulsive halogen and chalcogen lone-pairs and promotes the existence of an attractive *quasi*-linear three-body Br···Se–C_{Ph} fragment [169.59(1)°]. This has been classified as an attractive three-centre four electron type interaction resulting from the delocalisation of a halogen lone-pair (G) into the antibonding σ^* (Se–C) orbital.[29,30]

Conversely, CT adducts **4** and **5** display a notable increase in molecular distortion compared with donors **D2** and **D3**, respectively,[30] but naturally, adduct **4** containing the larger *peri*-moieties, exhibits the greatest degree of distortion. In both derivatives rotation around the Se(1)–C(1) bond aligns the Se–C_{Ph} bond in a twist conformation, thus altering the geometry from type BA, exhibited by **D2** and **D3**, to type CA-*c* (Fig. 3).[30,36] The geometry of the two acenaphthene ring systems, is dominated by the divergence of the *peri*-groups within the mean plane, though tilting of the E–C_{Acenap} bonds is more pronounced in **4** (splay angles: **4** 20.5°, **5** 19.0°). Correspondingly, Se···E *peri*-distances in the pair of CT adducts [**4** 3.326(3) Å; **5** 3.252 (2) Å] are notably longer than the respective donor compounds [**D2** 3.1834(10) Å; **D3** 3.113(4) Å],[30] only 12% shorter than the respective van der Waals radii (*cf.* **D2**/**D3** 16%).[30] Adversely, the *hypervalent* Se-I-I fragments in both compounds occupy a position pointing away from the *peri*-gap, contrasting with the geometry adopted by **1** and naphthalene analogues of **4** and **5**.[27] This is indicated by E···Se-I angles 128.41° (**4**) and 129.05° (**5**) (*cf.* **1** Br···Se-I 78.24°). Nevertheless, the Se-I vector lies *quasi*-perpendicular to the C(13)–Se(1)–C(1) plane due to steric crowding around the selenium lone-pairs [**4** θ = 79.27(1)°; **5** θ = 79.32(1)°; Fig. 2].[7] Additional weak non-covalent interactions exist within the crystal structures of **4** and **5**. The CA-*cis* orientation encourages the association of neighbouring phenyl ring systems through intramolecular nonbonded π-π stacking. Rotation around the Se–C_{Ph} bonds affords a mutual equatorial-axial arrangement of the phenyl rings with respect to the C_{Acenap}–E–C_{Ph} planes which promotes an edge-to-face motif, resulting from weak CH···π interactions.[37] CH···centroid (Cg) distances are in the range for typical CH···π edge-to-face π-stacking (3.0 Å).[38]

Further intermolecular CH···π short contacts exist between individual molecules within the molecular structures of **4** and **5**. The π···π interactions are illustrated in Fig. 4 and hydrogen bond data is displayed in Table S3†.

Crystallographic data suggests that dibromine addition products formed from diorganoselenium donor compounds exclusively adopt see-saw geometries, bearing a distinctive linear Br–Se–Br component.[7–9,39] We have recently reported the synthesis of two tribromide salts containing bromoselanyl cations [R_2Se–Br]$^+$, prepared from the naphthalene analogues of **D2** and **D3**, which do not adopt see-saw geometries and thus contradict the observed trend.[27] The reactivity of **D2** and **D3** mirrors that of the corresponding naphthalene donor compounds. Upon treatment with dibromine, the extensive electron donating ability of selenium affords a strong donor-strong acceptor system which subsequently weakens the dibromine bond. Partial negative charge, delocalised on the terminal Br atom encourages donation to a second dibromine molecule (acceptor).[7,8,27] The Se(1)–Br(1) bond is strengthened to such an extent that the Br(1)–Br(2) bond is cleaved and tribromide salts **2** and **3** result [R_2Se–Br]$^+$···

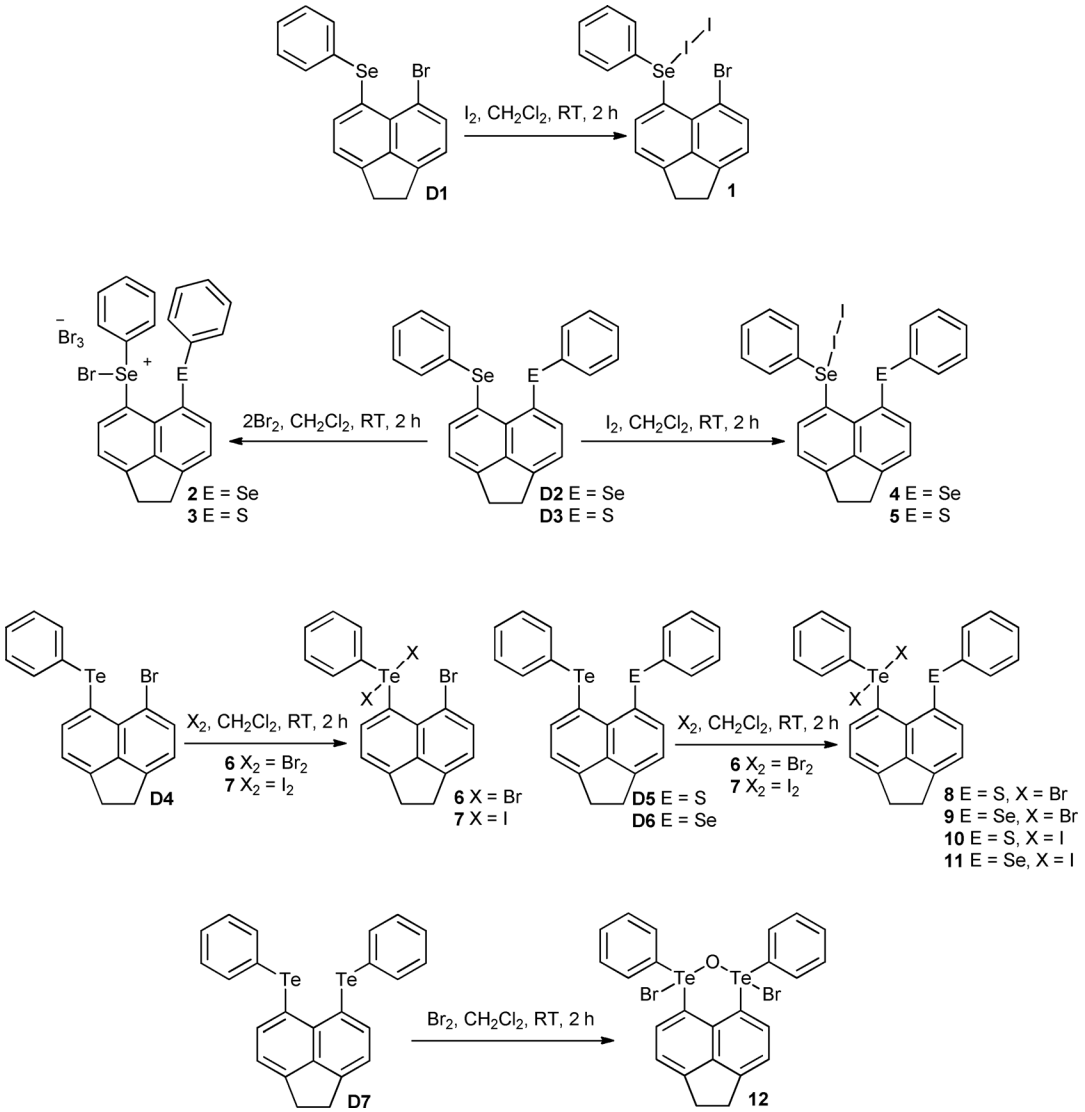

Scheme 1 The syntheses of addition products **1–12**, formed from the reactions of selenium and tellurium donors **D1–D7** with dibromine and diiodine.

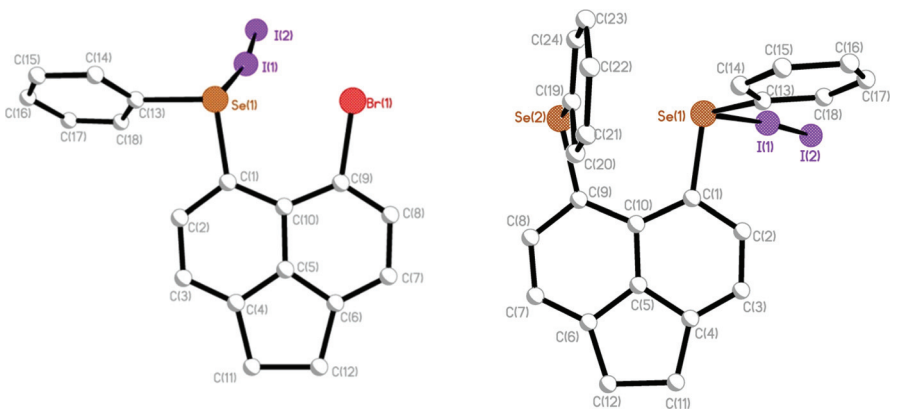

Fig. 1 The molecular structures of CT spoke adducts **1** and **4** (H atoms omitted for clarity). The structure of **5** (adopting a similar conformation to **4**) is omitted here but can be found in (Fig. S1†).

$[Br–Br_2]^-$ (Fig. 5).[7,8,27] The nature of the chemical bond in linear trihalide anions has been reviewed and classified by the Rundle and Pimentel model for electron rich 3c-4e systems and a charge-transfer model.[2,17] As expected, the Br–Br bonds in the *hypervalent quasi*-linear tribromide anions of **2** and **3** [**2** 178.19 (9)°; **3** 179.24(5)°] are weaker and subsequently longer

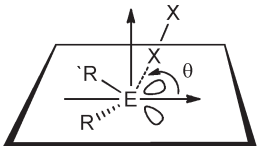

Fig. 2 Dihedral angle θ, defines the location of the dihalogen molecule and the geometry of CT spoke adducts formed from dihalogens binding to sp^3 hybridised chalcogen donor atoms.[7]

[2.50–2.62 Å; Table 3] than the bonding in free bromine [2.28 Å].[35]

The acenaphthene bromoselanyl cations of **2** and **3** adopt axial-axial conformations, aligning the E–C_{Ph} bonds perpendicular to the mean plane, with the phenyl rings assuming a *cis*-configuration (type AA-*c*; Fig. 3).[36] As a consequence of the geometry, the Br(1)–Se(1) bond lies equatorial with respect to the acenaphthene plane and by virtue forms a *quasi*-linear Br–Se···E′ three-body fragment [**2** 171.42°; **3** 174.95(1)°], which dominates the acenaphthene geometry. This can be thought of as a weak *hypervalent* G···Se-X 3c-4e type interaction, closely related to the T-shaped 3c-4e interaction, and has been shown to control the fine structures of compounds.[9]

Invariably, when large heteroatoms of Group 16 are constrained by a rigid organic backbone, such as acenaphthene or naphthalene, they experience considerable steric hindrance.[5,6,20] The repulsive interactions which consequently transpire between the two *peri*-functionalities as a result of their sub-van der Waals contacts, gives a natural preference for the carbon framework to distort from an ideal geometry.[18,19] This is achieved *via* in-plane and out-of-plane distortions of the exocyclic bonds and supplementary buckling of the aromatic ring system (angular strain).[5,6,20,21]

Alternatively, strain relief can be accomplished through attractive intramolecular interactions between *peri*-substituents due to the presence of weak or strong bonding, thus relaxing the geometry of the backbone without the need for molecular distortion.[6,20]

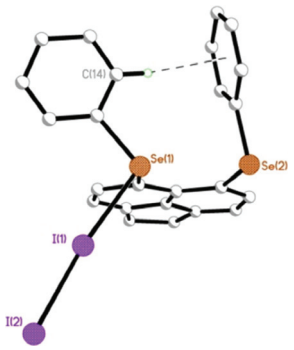

Fig. 4 Intramolecular (**4**) edge-to-face π-π stacking as a result of weak, hydrogen bond type, CH···π interactions.

Evidence of weak *hypervalent* E′···Se–Br 3c-4e type interactions operating in **2** and **3** comes from conspicuously short intramolecular Se···E′ *peri*-separations [**2** 2.801(3) Å] and [**3** 2.740(3) Å] compared with the non-bonding interactions observed in donors **D2** [3.1834(5) Å] and **D3** [3.113(4) Å].[30] These distances are 26% shorter than the sum of van der Waals radii for the two interacting atoms and approach the distances for single electron pair Se–Se/Se–S bonds [2.3639(5) Å; 2.24(1) Å].[27,40] This dramatic contraction is also accompanied by a natural reduction in molecular distortion, particularly within the acenaphthene plane where the divergence of exocyclic E–C_{Acenap} bonds is noticeably less pronounced (splay angles **2** 7.3°, **3** 5.4°; *cf.* **D2** 16.5°, **D3** 12.7°).[30]

It is therefore conceivable to predict that an attractive intramolecular non-covalent interaction exists between the two bulky chalcogen atoms in both cations to alleviate steric strain. The linear nature of the Br–Se···E′ fragments suggest these are weakly attractive *hypervalent* 3c-4e interactions,[2,9,17] which are found to prevail in analogous naphthalene systems.[28]

To complement these findings, density functional theory (DFT) calculations were performed for selected compounds of this study, calling special attention to the extent of chalcogen-chalcogen binding. Table 7 summarises selected geometrical

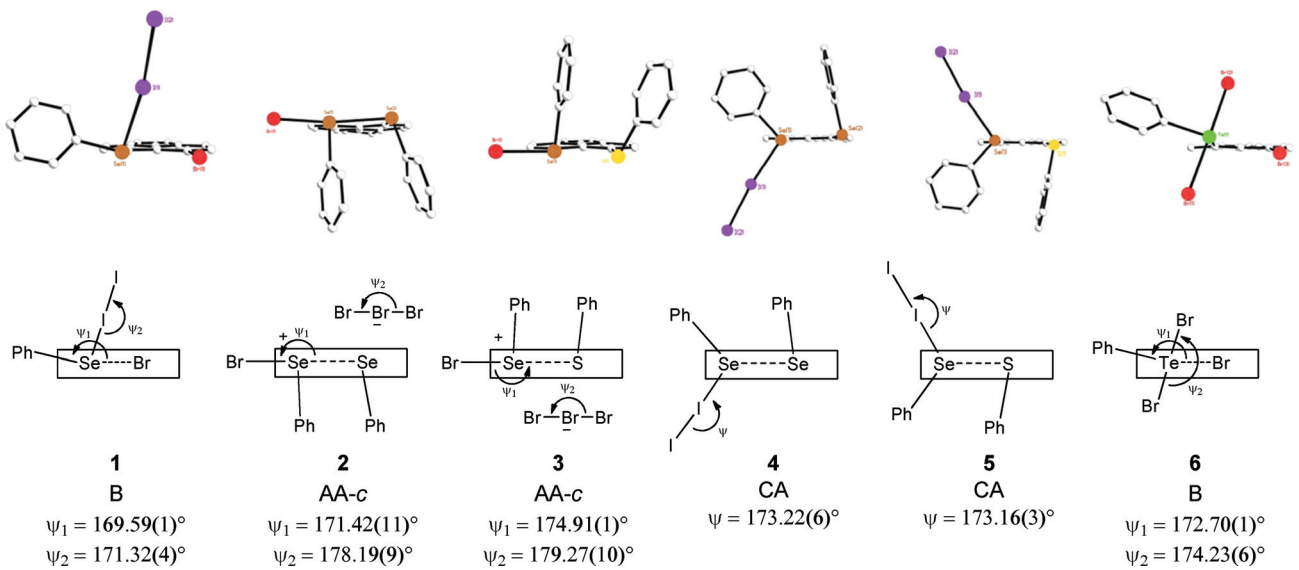

Fig. 3 The orientation of the E(phenyl) groups, the *quasi*-linear arrangements and structural conformations of **1–6**.

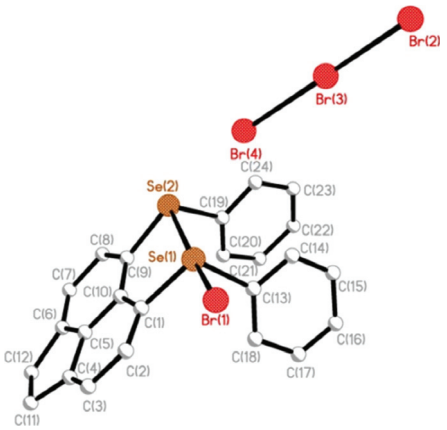

Fig. 5 The molecular structure of bromoselanyl tribromide salt **2** (H atoms omitted for clarity). The structure of **3** (adopting a similar conformation) is omitted here but can be found (Fig. S1†).

parameters for **2**, **3** and the corresponding bare cations **2a** and **3a**, together with the chalcogen-chalcogen Wiberg bond indices (WBIs).[41] The latter are a probe for the extent of covalent bonding, approaching a value close to one for true single bonds.

In all cases, significant WBIs between *ca.* 0.36 and 0.26 are obtained for the Se–Se or Se–S pairs (Table 7). The WBIs obtained for the Se–Br bonds are between 0.57 and 0.69, suggesting substantial 3c-4e character in these systems.

Even though the orientation of the Br_3^- moiety in the optimised isolated ion pairs differs somewhat from that observed in the periodic crystals, it is interesting to note that its presence appears to reinforce chalcogen-chalcogen bonding. This increased bonding is evidenced by a slight decrease in the Se···X distances (by *ca.* 0.06 Å to 0.08 Å) and a concomitant increase in the WBIs (by 0.04 to 0.06, compare data for **2** and **2a**, or for **3** and **3a** in Table 7). The computed values for the diselenium cation **2a** are similar to those of the corresponding naphthalene congeners[28] and in between those for the neutral acenaphthene species with two SePh groups[30] and with one[26] or two[42] Se–Br moieties (see Fig. 6).

Typically, see-saw or T-shaped molecular geometries are formed when the electronegativity of the halide is greater than that of the chalcogen donor species.[7–9] In this instance, nucleophilic halide attack occurs at the chalcogen atom of the intermediate $[R_2E^{\delta+}–X^{\delta-}]$ cation, affording a *hypervalent quasi*-linear X-E-X moiety.[7–9] Consequently, organotellurium

Table 7 Selected optimised distances [B3LYP/6-31+G* level, in Å] for **2**, **3**, together with the Se···X bond indices [WBIs, in brackets]. In italics: experimental data (XRD)[a]

Compound	*d*(Se···X)	[WBI]	*d*(Se···Br_3)	*d*(X···Br_3)
2a[b]	2.913	[0.304]	—	—
2	2.829	[0.364]	3.812	3.466
2	*2.801*	*[0.341]*	*3.53*	*3.868*
3a[b]	2.842	[0.256]	—	—
3	2.778	[0.295]	3.639	3.728
3	*2.74*	*[0.277]*	*3.67*	*3.973*

[a] Including WBIs calculated for the coordinates from X-ray crystallography; [b] **2a** and **3a** are bare cations, *i.e.* with the Br^{3-} counteranion deleted.

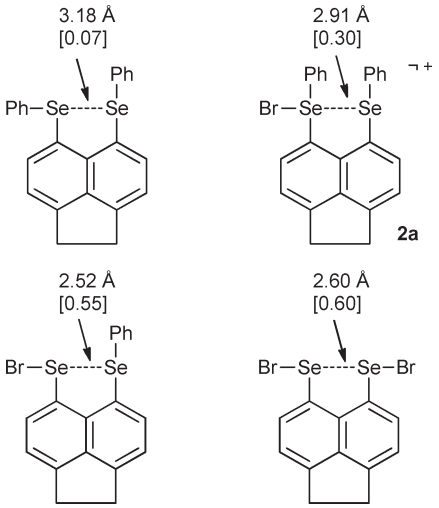

Fig. 6 B3LYP-computed Se···Se distances and WBIs [in brackets] in selected acenaphthene derivatives.

compounds [χ(Te) 2.08][32] are known to react with dihalogens and interhalogens [χ(F) 3.94–χ(I) 2.36][32] to form see-saw or T-shaped adducts, with no CT XY-adducts known for organic tellurium donors.[9] Tellurium forms strong donor-strong acceptor systems with the dihalogens, strong enough to cleave the X-X bond and oxidize tellurium.

Tellurium donors **D4–D6** react conventionally with dibromine and diiodine, affording a series of insertion adducts (**6–11**) exhibiting molecular see-saw geometries analogous to those of corresponding naphthalene adducts (Fig. 7).[9,28] In the mixed chalcogen species **D5** and **D6**, the addition reaction occurs exclusively at the tellurium site due to the greater donor ability of Te over Se/S. In each derivative, the linear X-Te-X moiety [172.7–177.7°] lies axial to the equatorial plane consisting of the two organo-groups and the lone pair on tellurium. Te–Br bond distances vary from 2.66–2.70 Å and Te–I distances from 2.89–2.96 Å, with a degree of asymmetry in some instances (*cf.* **10** Te(1)–I(1) 2.89, Te(1)–I(2) 2.96; Table 3). In each case, the tellurium atom adopts a distorted trigonal bipyramidal (TBP) geometry with angles around the central atom in the range 86.1–100.3° (Fig. 8).

The presence of the linear three-body system in **6–11** has no significant effect on the conformation of the phenyl rings, the acenaphthene configuration or the degree of molecular distortion compared with **D4–D6**.[30] Bromo compounds **6** and **7** adopt type B structures with an equatorial alignment of the Te–C_{Ph} bond with respect to the acenaphthene plane and mixed chalcogen compounds **8–11** adopt similar BA type structures (Fig. 8).[36]

In each tellurium derivative, a *quasi*-linear G···Te–C_{Ph} alignment exists with angles [159.6–176.6°] and intramolecular *peri*-distances 17–19% shorter than the sum of van der Waals radii [**6** 3.2581(19) Å; **7** 3.2050(11) Å; **8** 3.218(3) Å; **9** 3.2729(8) Å; **10** 3.141(4) Å; **11** 3.2677(18) Å (3.2862(18) Å)].

Whilst this linear alignment exhibits weak *hypervalent* 3c-4e character,[26,28,29] the interactions between *peri*-functionalities are minimal when compared with adducts **2** and **3**. The generation of the X-Te-X insertion fragment is accompanied by a prominent downfield shift in the ^{125}Te NMR spectra of **6–11** related to

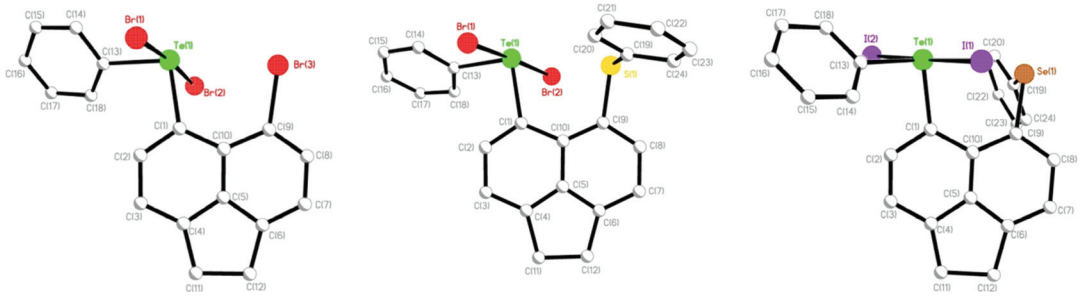

Fig. 7 The molecular see-saw geometry adopted in the structures of tellurium insertion adducts **6**, **8** and **11** (H atoms omitted for clarity). The structures of **7**, **9** and **10** (adopting conformations similar to **6**, **8** and **11**, respectively) are omitted here but can be found (Fig. S2†).

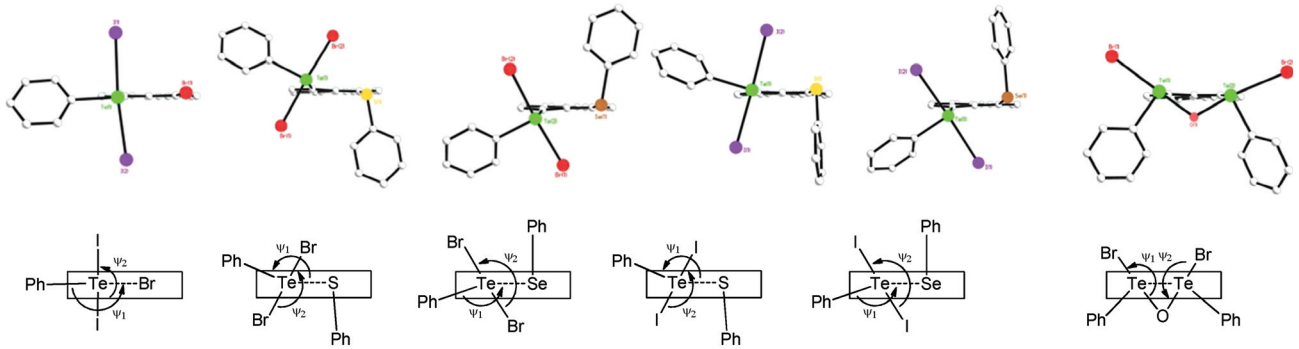

7	**8**	**9**	**10**	**11**	**12**
B	BA	BA	BA	BA	CC-*c*
ψ_1 = 176.55(1)°	ψ_1 = 162.26(1)°	ψ_1 = 162.18(1)°	ψ_1 = 161.77(1)°	ψ_1 = 159.62(1)°[164.44(1)°]	ψ_1 = 176.46(8)°[174.73(8)°]
ψ_2 = 173.04(2)°	ψ_2 = 175.49(7)°	ψ_2 = 175.54(3)°	ψ_2 = 177.73(4)°	ψ_2 = 177.18(4)°[177.67(4)°]	ψ_2 = 172.52(9)°[175.41(9)°]

Fig. 8 The orientation of the E(phenyl) groups, the *quasi*-linear arrangements and structural conformations of **7**–**12**.

D4–**D6** [δ = 696.0, 689.4, 663.4 ppm, respectively].[30] Single peaks are observed in all six spectra, with signals for bromine analogues **6** [δ = 918.8 ppm], **8** [δ = 930.6 ppm] and **9** [δ = 921.9 ppm], displaying higher chemical shifts than their iodine counterparts **7** [δ = 860.6 ppm], **10** [δ = 878.9 ppm] and **11** [δ = 871.0 ppm].

Additional weak non-covalent interactions exist between individual molecules within the crystal structures of **6**–**11**; CH···π interactions[37] range from 2.69–2.96 Å within the known CH···centroid (Cg) range[38] and a number of short CH···X hydrogen bond type interactions are also present (H···Br 2.66–2.94 Å; H···I 3.03–3.05 Å; see Table S3 †. Further short intermolecular contacts exist between Te and I atoms of neighbouring I–Te–I units in **10** constructing a planar Te_2I_2 square with Te···I distances of 3.925(1) Å.

Generally, when tellurium donors are treated with dihalogen or interhalogen acceptors, see-saw or T-shaped molecular geometries are observed, characterised by *hypervalent* X-Te-X fragments.[9] In contrast, the di-tellurium donor **D7** reacts with a single equivalent of dibromine to afford the insertion see-saw adduct **12**, exhibiting an unexpected Te–O–Te bridge, two *quasi*-linear Br–Te–O fragments and no classical Br–Te–Br moiety (Fig. 9). Repeating the reaction under standard Schlenk conditions and with a higher loading of dibromine had no effect on the outcome of the reaction, exclusively affording **12** each time and indicating the origin of the oxygen atom was the parent dibromine solution. In order to explore the reason why bromination of Acenap$(TePh)_2$ results exclusively in the oxygenated derivative **12**, rather than in pure organotellurium bromides, additional DFT computations were performed. Products that could have been expected comprise **Ax**, the analogue of the known compounds Acenap$(TePhBr_2)$(EPh) (E = S, Se),[28] **Ay1**, a doubly brominated species, and **Ay2**, the congener of **2** (Fig. 10).

The optimised geometries of these possible products are unremarkable, with Te···Te distances of 3.44 Å [0.15], 3.84 Å [0.01], and 3.04 Å [0.48] for **Ax**, **Ay1**, and **Ay2**, respectively [WBIs in brackets]. **Ay1** has two unsymmetric Te–Br···Te bridges (Te–Br

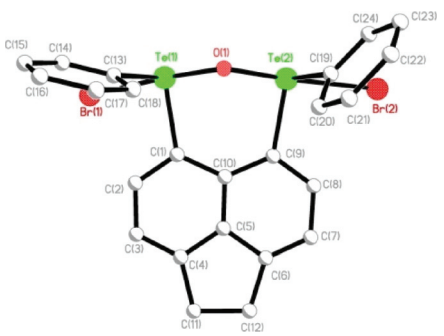

Fig. 9 The molecular structure of tellurium insertion adduct **12** (H atoms omitted for clarity).

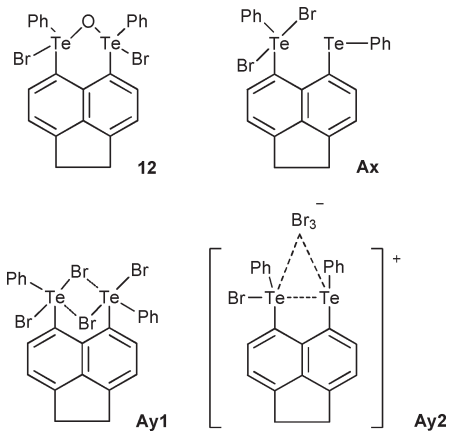

Fig. 10 Possible products from the reaction of Acenap(TePh)$_2$ **D7** and dibromine.

and Te···Br distances of 2.81 Å and 3.47 Å, respectively), but is otherwise similar to the known, more symmetric $ArBr_2Te(\mu\text{-}Br)_2TeBr_2Ar$ (Ar = *p*-C_6H_4OMe).[43]

The structure of the actual product, **12**, is more complicated, as it forms dimers in the crystal, denoted (**12**)$_2$ in the following. A monomeric minimum **12** can be optimised, in which the roughly linear Br–Te–O moieties of the dimer are preserved. A similar structure with an isosceles BrTe–O–TeBr triangle is found in (nBu)$_2$BrTe–O–TeBr(nBu)$_2$,[44] albeit with a wider Te–O–Te bond angle, 122.4° (*cf.* 111.5° and 118.3° in **12** and (**12**)$_2$, respectively, mean expt. 114.6°). As expected, little direct Te–Te bonding is apparent in **12** and (**12**)$_2$, despite the rather short Te···Te contacts of 3.38 Å and 3.49 Å, respectively (*cf.* mean expt. 3.36 Å, all WBIs 0.02).

Selected reaction energies are collected in Table 8, including corrections for entropy and environment effects. The latter are assessed through a polarisable continuum modelling a solvent of medium polarity, dichloromethane (for compatibility with our previous results for related Se complexes).[28] In the following, we discuss primarily the $\Delta G_r(CH_2Cl_2)$/B3LYP-D3 data (last column in Table 8). Reaction (1), *i.e.* formation of **Ax**, has the largest computed driving force. A second bromination yielding **Ay1**, reaction (2), is much less favourable. Ionic **Ay2** is predicted to be endothermic throughout, consistent with the failure to observe it experimentally. Assuming that water is the most likely source for the O atom in **12**, reaction (4) is a plausible channel leading to the latter. Formation of monomeric **12** through this path is predicted to be unfavourable throughout, by at least 7.8 kcal mol^{-1}. Dimerisation of **12** appears to be mainly driven by dispersion (compare the last two $\Delta G_r(CH_2Cl_2)$ values in Table 8), but with a very low overall driving force. Notwithstanding the crude nature of some approximations involved (ideal-gas entropies, continuum solvation model), (**12**)$_2$ does not appear to be a deep thermodynamic sink. Its formation according to reactions (4) and (5) is viable under the experimental conditions, when the other product, HBr, is removed from the equilibrium mixture through vaporisation.

The formation of the two Br–Te–O fragments is accompanied by a prominent downfield shift in the ^{125}Te NMR spectrum of **12** compared to donor **D7** [δ = 585.9 ppm] with a single peak at δ = 961.3 ppm.

The see-saw molecular geometry ensures the central tellurium atoms occupy similar distorted trigonal bipyramidal (TBP) environments [84.0–96.5°], with both linear Br–Te–O moieties [172.5–176.5°] lying axial to the equatorial planes formed by the tellurium organo-groups and lone pairs. The two Br–Te–O fragments lie *quasi*-perpendicular to one another, the oxygen atom forced into a distorted angular geometry, with a Te–O–Te angle of 113.11(15)° [116.17(16)°].

Interestingly, the degree of molecular distortion in **12** is comparable to donor **D7**,[30] with an intramolecular Te···Te *peri*-separation of 3.335(1) Å [3.385(1) Å], ~19% shorter than the sum of van der Waals radii (*cf.* **D7** 3.3674(19) Å; 18%).[30] The large tellurium atoms are accommodated by a significant in-plane distortion of the exocyclic Te–C_{Acenap} bonds, with a large angular splay of 19.0° [20.1°]. Conversely, only a small displacement of the *peri*-atoms is observed from the mean acenaphthene plane, with Te(1) 0.05(1) Å [0.10(1) Å] and Te(2) 0.14(1) Å [0.12(1) Å] from the plane respectively. The twist alignment of the two Te–C_{Ph} bonds, *cis* to the mean acenaphthene plane (type CC-*c*; Fig. 8),[36] implies there is no phenyl ring overlap and no π-stacking, however a number of short intermolecular interactions exist between Br and Te atoms of neighbouring Br–Te–O units (Br···Te 3.32–3.68 Å). Br–Te bond lengths 2.77–3.02 Å are all longer than expected[45] and longer than the bond lengths observed in **6–11**, with the Br(3)–Te(3) bond distance in the second independent molecule significantly longer at 3.024(7) Å. Te–O bond lengths 1.94–2.05 Å are at the lower end of the range for known Br–Te–O fragments.[45]

Conclusion

The group of selenium and tellurium acenaphthene donors **D1–D7** [Acenap(EPh)(Br) E = Se, Te; Acenap(SePh)(EPh) E = Se, S; Acenap(TePh)(EPh) E = S, Se, Te] have been reacted with dihalogens, dibromine and diiodine, to afford a range of

Table 8 Selected reaction energies and free energies [in kcal mol^{-1}] at the B3LYP level, except where otherwise noted

Reaction	ΔE_r	ΔE_r+ZPE^a	$\Delta G_r^{298\ K}$	$\Delta G_r(CH_2Cl_2)$	$\Delta G_r(CH_2Cl_2)$ B3LYP-D3^b
(1) Acenap(TePh)2 + Br_2 → **Ax**	−16	−14.9	−2.9	−7.1	−18.7
(2) **Ax** + Br_2 → **Ay1**	−1.5	−0.8	10.8	5.4	−4.8
(3) **Ay1** → **Ay2**	15.7	15.4	13.6	5	7.9
(4) **Ax** + Br_2 + H_2O → **12** + 2 HBr	12.5	8.4	10.6	8.3	7.8
(5) 2 **12** → (**12**)$_2$^{c}	−6.4	−6.4	5.3	11.7	−1.6

^{a} Including zero-point energy. ^{b} Including an empirical dispersion correction. ^{c} Including BSSE correction.

structurally diverse addition products. Selenium donors **D1–D3** reacted conventionally with diiodine forming three neutral charge-transfer (CT) spoke adducts (R_2E-X-Y, 10-X-2) **1**, **4** and **5**, characterised by *hypervalent* three-body Se-I-I linear fragments. In each case, upon coordination of selenium to the diiodine molecule, no significant alteration to the acenaphthene geometry was observed compared with the respective donor compounds.

Conversely, when selenium donors **D2** and **D3** were treated with dibromine, two tribromide salts containing bromoselanyl cations $[R_2Se–Br]^+$ were afforded, similar to the reactions of corresponding naphthalene donors. In both adducts, the geometry of the bromoselanyl cation is dominated by a *quasi*-linear Br–Se···E′ three-body fragment, resulting from the *cis*-orientation of axial phenyl rings with respect to the mean acenaphthene plane (type AA-*c*). The combination of conspicuously short intramolecular Se···E′ *peri*-separations (26% shorter than the sum of van der Waals radii) and angles that approach 180°, implies a weak *hypervalent* G···Se–X 3c-4e type interaction operates within the linear three-body systems. Density functional theory (DFT) calculations performed on **2**, **3** and their bare cations **2a** and **3a**, support this interpretation; WBIs were obtained between *ca.* 0.26 and 0.36 in all four cases, with computed values for di-selenium cation **2a**, similar to the corresponding naphthalene congener and in between those of the neutral donor species **D2** [WBI 0.07] and acenaphthene species with one[26] [WBI 0.55] or two[52] [WBI 0.60] Se-Br moieties. Further evidence of an attractive *peri*-interaction operating in **2** and **3** is the substantial reduction in molecular distortion observed in the acenaphthene geometry compared with respective donor compounds.

Treatment of tellurium donors **D4–D6** with dibromine and diiodine afforded a series of typical insertion adducts (**6–11**) exhibiting molecular see-saw geometries, distinguished by *quasi*-linear *hypervalent* X–Te–X functionalities. In the mixed chalcogen species **D5** and **D6**, the addition reaction occurred exclusively at the tellurium site due to the greater donor ability of Te over Se/S. Acenaphthene distortion in all six compounds is comparable with donors **D4–D6** and no significant attractive interaction is observed between the *peri*-substituents.

Conversely, ditellurium donor **D7** reacted with dibromine to afford an unusual oxygenated derivative, containing a Te–O–Te bridge and two *quasi*-linear Br–Te–O fragments. Further reactions performed under standard Schlenk conditions and with a higher loading of dibromine had no effect on the outcome and exclusively afforded **12** each time. In order to understand why the oxygenated derivative is favoured over more conventional pure organotellurium bromides, additional DFT computations were performed for possible products of the reaction. Whilst **12** was found to be the least thermodynamically favourable of a series of potential products, its formation is viable under experimental conditions following the removal of HBr from the system. Despite the short Te···Te contacts in **12**, no direct Te–Te bonding is apparent [WBIs 0.02].

Acknowledgements

Elemental analyses were performed by Sylvia Williamson, Donna McColl and Stephen Boyer. Mass Spectrometry was performed by Caroline Horsburgh. Calculations were performed using the EaStCHEM Research Computing Facility maintained by Dr H. Früchtl. The work in this project was supported by the Engineering and Physical Sciences Research Council (EPSRC). Michael Bühl wishes to thank EaStCHEM and the University of St Andrews for support.

Notes and references

1 G. N. Lewis, in *Valence and the Structure of Atoms and Molecules*, The Chemical Catalog Co., New York, 1923, ch. 8; I. Langmuir, *Science*, 1921, **54**, 59.

2 J. J. Hatch and R. E. Rundle, *J. Am. Chem. Soc.*, 1951, **73**, 4321; R. E. Rundle, *J. Am. Chem. Soc.*, 1963, **85**, 112; R. E. Rundle, *J. Am. Chem. Soc.*, 1947, **69**, 1327; S. Sugden, in *The Parachor and Valency*, Knopf, New York, 1930, ch. 6; G. C. Pimental, *J. Chem. Phys.*, 1951, **19**, 446.

3 L. Pauling, in *The Nature of the Chemical Bond*, ed. L. Pauling, Cornell University Press, Ithaca, New York, 3rd edn, 1960, ch. 7; L. Pauling, *J. Am. Chem. Soc.*, 1947, **69**, 542.

4 C. A. Coulson, d-Orbitals in Chemical Bonding, in *Proceedings of the Robert A. Welch Foundation Conferences on Chemical Research. XVI. Theoretical Chemistry*, ed. W. O. Mulligen, Houston, Texas, 1972, ch. 3; T. B. Brill, *J. Chem. Educ.*, 1973, **50**, 392; W. Kutzelnigg, *Angew. Chem., Int. Ed. Engl.*, 1984, **23**, 272; *Valency and Bonding*, ed. F. Weinhold and C. Landis, Cambridge University Press, Cambridge, UK, 2005, ch. 3.

5 For example: H. E. Katz, *J. Am. Chem. Soc.*, 1985, **107**, 1420; R. W. Alder, P. S. Bowman, W. R. S. Steel and D. R. Winterman, *Chem. Commun.*, 1968, 723–4; T. Costa and H. Schimdbaur, *Chem. Ber.*, 1982, **115**, 1374; A. Karacar, M. Freytag, H. Thönnessen, J. Omelanczuk, P. G. Jones, R. Bartsch and R. Schmutzler, *Heteroat. Chem.*, 2001, **12**, 102; J. Meinwald, D. Dauplaise, F. Wudl and J. J. Hauser, *J. Am. Chem. Soc.*, 1977, **99**, 255; R. S. Glass, S. W. Andruski, J. L. Broeker, H. Firouzabadi, L. K. Steffen and G. S. Wilson, *J. Am. Chem. Soc.*, 1989, **111**, 4036; T. Fuji, T. Kimura and N. Furukawa, *Tetrahedron Lett.*, 1995, **36**, 1075; G. P. Schiemenz, *Z. Anorg. Allg. Chem.*, 2002, **628**, 2597; R. J. P. Corriu and J. C. Young, Hypervalent Silicon Compounds, in *Organic Silicon Compounds*, ed. S. Patai and Z. Rappoport, John Wiley & Sons Ltd, Chichester, UK, 1989, vol. 1 and 2.

6 W. Nakanishi, S. Hayashi and S. Toyota, *Chem. Commun.*, 1996, 371; W. Nakanishi, S. Hayashi, A. Sakaue, G. Ono and Y. Kawada, *J. Am. Chem. Soc.*, 1998, **120**, 3635; W. Nakanishi, S. Hayashi and S. Toyota, *J. Org. Chem.*, 1998, **63**, 8790; S. Hayashi and W. Nakanishi, *J. Org. Chem.*, 1999, **64**, 6688; W. Nakanishi, S. Hayashi and T. Uehara, *J. Phys. Chem. A*, 1999, **103**, 9906; W. Nakanishi, S. Hayashi and T. Uehara, *Eur. J. Org. Chem.*, 2001, 3933; W. Nakanishi and S. Hayashi, *Phosphorus, Sulfur Silicon Relat. Elem.*, 2002, **177**, 1833; W. Nakanishi, S. Hayashi and T. Arai, *Chem. Commun.*, 2002, 2416; S. Hayashi and W. Nakanishi, *J. Org. Chem.*, 2002, **67**, 38; W. Nakanishi, S. Hayashi and N. Itoh, *Chem. Commun.*, 2003, 124; S. Hayashi, H. Wada, T. Ueno and W. Nakanishi, *J. Org. Chem.*, 2006, **71**, 5574; S. Hayashi and W. Nakanishi, *Bull. Chem. Soc. Jpn.*, 2008, **81**, 1605.

7 V. Lippolis and F. Isaia, in *Handbook of Chalcogen Chemistry*, ed. F. A. Devillanova, RSC Publishing: Cambridge, 2007, ch. 8.2 and references cited therein.

8 P. D. Boyle and S. M. Godfrey, *Coord. Chem. Rev.*, 2001, **223**, 265 and references cited therein.

9 W. Nakanishi, in *Handbook of Chalcogen Chemistry, New Perspectives in Sulfur, Selenium and Tellurium*, ed. F. A. Devillanova, RSC Publishing, Cambridge, 2007, ch. 10.3 and references cited therein.

10 For example: M. C. Aragoni, M. Arca, F. Demartin, F. A. Devillanova, A. Garau, F. Isaia, V. Lippolis and G. Verani, *J. Am. Chem. Soc.*, 2002, **124**, 4538; M. C. Aragoni, M. Arca, F. A. Devillanova, F. Isaia, V. Lippolis, A. Mancini, L. Pala, A. M. Z. Slawin and J. D. Woollins, *Chem. Commun.*, 2003, 2226; F. Demartin, P. Deplano, F. A. Devillanova, F. Isaia, V. Lippolis and G. Verani, *Inorg. Chem.*, 1993, **32**, 3694; F. Bigoli, F. Demartin, P. Deplano, F. A. Devillanova, F. Isaia, V. Lippolis, M. L. Mercuri, M. A. Pellinghelli and E. F. Trogu, *Inorg. Chem.*, 1996, **35**, 3194; M. C. Aragoni, M. Arca, F. Demartin, F. A. Devillanova, A. Garau, F. Isaia, V. Lippolis and G. Verani, *Trends Inorg. Chem.*, 1999, **6**, 1 and references cited therein.

11 W. Nakanishi, S. Hayashi and H. Kihara, *J. Org. Chem.*, 1999, **64**, 2630.

12 W. Nakanishi, S. Hayashi, H. Tukada and H. Iwamura, *J. Phys. Org. Chem.*, 1990, **3**, 358; W. Nakanishi, Y. Yamamoto, S. Hayashi, H. Tukada and H. Iwamura, *J. Phys. Org. Chem.*, 1990, **3**, 369; W. Nakanishi and S. Hayashi, *J. Organomet. Chem.*, 2000, **611**, 178; W. Nakanishi and S. Hayashi, *Heteroat. Chem.*, 2001, **12**, 369; W. Nakanishi, S. Hayashi and Y. Kusuyama, *J. Chem. Soc., Perkin Trans. 2*, 2002, 262; P. H. Laur, S. M. Saberi-Niaki, M. Scheiter, C. Hu, U. Englert, Y. Wang and J. Fleischhauer, *Phosphorus, Sulfur Silicon Relat. Elem.*, 2005, **180**, 1035.

13 M. D. Rudd, S. V. Linderman and S. Husebye, *Acta Chem. Scand.*, 1997, **51**, 689.

14 M. C. Aragoni, M. Arca, F. Demartin, F. A. Devillanova, A. Garau, F. Isaia, F. Lelj, V. Lippolis and G. Verani, *Chem. Eur. J.*, 2001, **7**, 3122; M. C. Aragoni, M. Arca, F. Demartin, F. A. Devillanova, A. Garau, F. Isaia, V. Lippolis and G. Verani, *Dalton Trans.*, 2005, 2252.

15 M. C. Baenziger, R. E. Buckles, R. J. Maner and T. D. Simpson, *J. Am. Chem. Soc.*, 1969, **91**, 5749.

16 *Chemistry of Hypervalent Compounds*, ed. K.-Y. Akiba, Wiley-VCH, New York, NY, USA, 1999; G. A. Landrum, N. Goldberg and R. Hoffmann, *J. Chem. Soc., Dalton Trans.*, 1997, 3605; P. H. Svensson and L. Kloo, *Chem. Rev.*, 2003, **103**, 1649; C. W. Perkins, J. C. Martin, A. J. Arduengo, W. Law, A. Alegrie and J. K. Kocki, *J. Am. Chem. Soc.*, 1980, **102**, 7753.

17 M. C. Aragoni, M. Arca, F. Demartin, F. A. Devillanova, A. Garau, F. Isaia, V. Lippolis and A. Mancini, *Bioinorg. Chem. Appl.*, 2007, **2007**, 17416.

18 C. A. Coulson, R. Daudel and J. M. Robertson, *Proc. R. Soc. London, Ser. A*, 1951, **207**, 306; D. W. Cruickshank, *Acta Crystallogr.*, 1957, **10**, 504; C. P. Brock and J. D. Dunitz, *Acta Crystallogr. Sect. B*, 1982, **38**, 2218; J. Oddershede and S. Larsen, *J. Phys. Chem. A*, 2004, **108**, 1057.

19 A. C. Hazell, R. G. Hazell, L. Norskov-Lauritsen, C. E. Briant and D. W. Jones, *Acta Crystallogr., Sect. C*, 1986, **42**, 690.

20 V. Balasubramaniyan, *Chem. Rev.*, 1966, **66**, 567.

21 H. Schmidbaur, H.-J. Öller, D. L. Wilkinson, B. Huber and G. Müller, *Chem. Ber.*, 1989, **122**, 31; H. Fujihara and N. Furukawa, *J. Mol. Struct.*, 1989, **186**, 261; H. Fujihara, R. Akaishi, T. Erata and N. Furukawa, *J. Chem. Soc., Chem. Commun.*, 1989, 1789; J. Handal, J. G. White, R. W. Franck, Y. H. Yuh and N. L. Allinger, *J. Am. Chem. Soc.*, 1977, **99**, 3345; J. F. Blount, F. Cozzi, J. R. Damewood, D. L. Iroff, U. Sjöstrand and K. Mislow, *J. Am. Chem. Soc.*, 1980, **102**, 99; F. A. L. Anet, D. Donovan, U. Sjöstrand, F. Cozzi and K. Mislow, *J. Am. Chem. Soc.*, 1980, **102**, 1748; W. D. Hounshell, F. A. L. Anet, F. Cozzi, J. R. Damewood, Jr., C. A. Johnson, U. Sjöstrand and K. Mislow, *J. Am. Chem. Soc.*, 1980, **102**, 5941; R. Schröck, K. Angermaier, A. Sladek and H. Schmidbaur, *Organometallics*, 1994, **13**, 3399.

22 P. Kilian, F. R. Knight and J. D. Woollins, *Chem. Eur. J.*, 2011, **17**, 2302; P. Kilian, F. R. Knight and J. D. Woollins, *Coord. Chem. Rev.*, 2011, **255**, 1387.

23 S. M. Aucott, H. L. Milton, S. D. Robertson, A. M. Z. Slawin, G. D. Walker and J. D. Woollins, *Chem. Eur. J.*, 2004, **10**, 1666; S. M. Aucott, H. L. Milton, S. D. Robertson, A. M. Z. Slawin and J. D. Woollins, *Heteroat. Chem.*, 2004, **15**, 531; S. M. Aucott, H. L. Milton, S. D. Robertson, A. M. Z. Slawin and J. D. Woollins, *Dalton Trans.*, 2004, **44**, 3347; S. M. Aucott, P. Kilian, H. L. Milton, S. D. Robertson, A. M. Z. Slawin and J. D. Woollins, *Inorg. Chem.*, 2005, 2710; S. M. Aucott, P. Kilian, S. D. Robertson, A. M. Z. Slawin and J. D. Woollins, *Chem. Eur. J.*, 2006, **12**, 895; S. M. Aucott, D. Duerden, Y. Li, A. M. Z. Slawin and J. D. Woollins, *Chem. Eur. J.*, 2006, **12**, 5495.

24 P. Kilian, A. M. Z. Slawin and J. D. Woollins, *Dalton Trans.*, 2003, 3876; P. Kilian, D. Philp, A. M. Z. Slawin and J. D. Woollins, *Eur. J. Inorg. Chem.*, 2003, **9**, 249; P. Kilian, A. M. Z. Slawin and J. D. Woollins, *Chem. Eur. J.*, 2003, 215; P. Kilian, A. M. Z. Slawin and J. D. Woollins, *Chem. Commun.*, 2003, 1174; P. Kilian, A. M. Z. Slawin and J. D. Woollins, *Dalton Trans.*, 2003, 3876; P. Kilian, H. L. Milton, A. M. Z. Slawin and J. D. Woollins, *Inorg. Chem.*, 2004, **43**, 2252; P. Kilian, A. M. Z. Slawin and J. D. Woollins, *Inorg. Chim. Acta*, 2005, **358**, 1719; P. Kilian, A. M. Z. Slawin and J. D. Woollins, *Dalton Trans.*, 2006, 2175.

25 F. R. Knight, A. L. Fuller, A. M. Z. Slawin and J. D. Woollins, *Dalton Trans.*, 2009, 8476; A. L. Fuller, F. R. Knight, A. M. Z. Slawin and J. D. Woollins, *Polyhedron*, 2010, **29**, 1849; A. L. Fuller, F. R. Knight, A. M. Z. Slawin and J. D. Woollins, *Polyhedron*, 2010, **29**, 1956; A. L. Fuller, F. R. Knight, A. M. Z. Slawin and J. D. Woollins, *Chem. Eur. J.*, 2010, **16**, 7617.

26 F. R. Knight, A. L. Fuller, M. Bühl, A. M. Z. Slawin and J. D. Woollins, *Chem. Eur. J.*, 2010, **16**, 7503.

27 A. L. Fuller, F. R. Knight, A. M. Z. Slawin and J. D. Woollins, *Eur. J. Inorg. Chem.*, 2010, 4034.

28 F. R. Knight, A. L. Fuller, M. Bühl, A. M. Z. Slawin and J. D. Woollins, *Inorg. Chem.*, 2010, **49**, 7577.

29 F. R. Knight, A. L. Fuller, M. Bühl, A. M. Z. Slawin and J. D. Woollins, *Chem. Eur. J.*, 2010, **16**, 7605; A. L. Fuller, F. R. Knight, A. M. Z. Slawin and J. D. Woollins, *Acta Crystallogr., Sect. E*, 2007, **E63**, o3855; A. L. Fuller, F. R. Knight, A. M. Z. Slawin and J. D. Woollins, *Acta Crystallogr., Sect. E*, 2007, **E63**, o3957; A. L. Fuller, F. R. Knight, A. M. Z. Slawin and J. D. Woollins, *Acta Crystallogr., Sect. E*, 2008, **E64**, o977.

30 L. K. Aschenbach, F. R. Knight, R. A. M. Randall, D. B. Cordes, A. Baggott, M. Bühl, A. M. Z. Slawin and J. D. Woollins, *Dalton Trans.*, 2012, DOI: 10.1039/C1DT11697E in press.

31 For example: D. W. Allen, R. Berridge, N. Bricklebank, S. D. Forder, F. Palacio, S. J. Coles, M. B. Hursthouse and P. J. Skabara, *Inorg. Chem.*, 2003, **42**, 3975; F. Bigoli, P. Deplano, M. L. Mercuri, M. A. Pellinghelli, A. Sabatini, E. F. Trogu and A. Vacca, *J. Chem. Soc., Dalton Trans.*, 1996, 3583; A. J. Blake, F. A. Devillanova, A. Garau, L. M. Gilby, R. O. Gould, F. Isaia, V. Lippolis, S. Parsons, C. Radek and M. Schröder, *J. Chem. Soc., Dalton Trans.*, 1998, 2037; M. Arca, F. Demartin, F. A. Devillanova, A. Garau, F. Isaia, V. Lippolis and G. Verani, *J. Chem. Soc., Dalton Trans.*, 1999, 3069; H. Hartl and S. Steidl, *Z. Naturforsch. B, Chem. Sci.*, 1977, **32**, 6; E. J. Lyon, G. Musie, J. H. Reibenspies and M. Y. Darensbourg, *Inorg. Chem.*, 1998, **37**, 6942.

32 A. L. Allred and E. G. Rochow, *J. Inorg. Nucl. Chem.*, 1958, **5**, 264; A. L. Allred and E. G. Rochow, *J. Inorg. Nucl. Chem.*, 1958, **5**, 269.

33 G. Y. Chao and J. D. McCullough, *Acta Crystallogr.*, 1961, **14**, 940; H. Hope and J. D. McCullough, *Acta Crystallogr.*, 1962, **15**, 806; H. Hope and J. D. McCullough, *Acta Crystallogr.*, 1964, **17**, 712; H. Maddox and J. D. McCullough, *Inorg. Chem.*, 1966, **5**, 522; J. Jeske, W.-W. du Mont and P. G. Jones, *Chem. Eur. J.*, 1999, **5**, 385; F. Cristiani, F. Demartin, F. A. Devillanova, F. Isaia, G. Saba and G. Verani, *J. Chem. Soc., Dalton Trans.*, 1992, 3553; S. M. Godfrey, C. A. McAuliffe, R. G. Pritchard and S. Sarwar, *J. Chem. Soc., Dalton Trans.*, 1997, 1031.

34 A. Bondi, *J. Phys. Chem.*, 1964, **68**, 441.

35 *Chemistry of the Elements*, ed. N. N. Greenwood and A. Earnshaw, Reed Elsevier, Oxford, 1997.

36 P. Nagy, D. Szabó, I. Kapovits, Á. Kucsman, G. Argay and A. Kálmán, *J. Mol. Struct.*, 2002, **606**, 61; W. Nakanishi and S. Hayashi, *J. Org. Chem.*, 2002, **67**, 38; S. Hayashi, K. Yamane and W. Nakanishi, *J. Org. Chem.*, 2007, **72**, 7587; W. Nakanishi, S. Hayashi and S. Toyota, *J. Am. Chem. Soc.*, 1998, **63**, 8790; W. Nakanishi, S. Hayashi and T. Uehara, *J. Phys. Chem.*, 1999, **103**, 9906; W. Nakanishi, S. Hayashi and T. Uehara, *Eur. J. Org. Chem.*, 2001, 3933.

37 M. Nishio, *CrystEngComm*, 2004, **6**, 130; C. Fischer, T. Gruber, W. Seichter, D. Schindler and E. Weber, *Acta Crystallogr. Sect. E*, 2008, **64**, o673; M. Hirota, K. Sakaibara, H. Suezawa, T. Yuzuri, E. Ankai and M. Nishio, *J. Phys. Org. Chem.*, 2000, **13**, 620; H. Tsubaki, S. Tohyama, K. Koike, H. Saitoh and O. Ishitani, *Dalton Trans.*, 2005, 385.

38 PLATON: A. L. Spek, *J. Appl. Crystallogr.*, 2003, **36**, 7; A. L. Spek, *Acta Crystallogr., Sect. D: Biol. Crystallogr.*, 2009, **D65**, 148.

39 S. M. Godfrey, C. A. McAuliffe, R. G. Pritchard and S. Sarwar, *J. Chem. Soc., Dalton Trans.*, 1997, 1031; J. D. McCullough and R. E. Marsh, *Acta Crystallogr.*, 1950, **3**, 41; M. Barlow and I. Zimmermann-Barlow, *Acta Chem. Scand. (Moscow Abstracts)*, 1966, **21**, A103; L. Battelle, C. Knobler and J. D. McCullough, *Inorg. Chem.*, 1967, **6**, 958; J. D. McCullough and G. Hamburger, *J. Am. Chem. Soc.*, 1941, **63**, 803.

40 J. Meinwald, D. Dauplaise and J. Clardy, *J. Am. Chem. Soc.*, 1977, **99**, 7743.

41 K. B. Wiberg, *Tetrahedron*, 1968, **24**, 1083.

42 M. Bühl, P. Kilian and J. D. Woollins, *ChemPhysChem*, 2011, **12**, 2405.

43 P. H. Bird, V. Kumar and B. C. Pant, *Inorg. Chem.*, 1980, **19**, 2487.

44 Z.-Z. Huang, S. Ye, W. Xia, Y.-H. Yu and Y. Tang, *J. Org. Chem.*, 2001, **67**, 3096.

45 CSD Version 5.32, Conquest 1.13 & Vista http://www.ccdc.cam.ac.uk/ (accessed June 2011).